Distribution Agreement

In presenting this thesis as a partial fulfillment of the requirements for a degree from Emory University, I hereby grant to Emory University and its agents the non-exclusive license to archive, make accessible, and display my thesis in whole or in part in all forms of media, now or hereafter know, including display on the World Wide Web. I understand that I may select some access restrictions as part of the online submission of this thesis. I retain all ownership rights to the copyright of the thesis. I also retain the right to use in future works (such as articles or books) all or part of this thesis.

Suk Whan Yoon

Date: 29 March 2012

Effect of Thermal Conditions and Mechanical Stress During Vitrification on Physical Aging of Thin Polymer Films

by

Suk Whan Yoon

Dr. Connie B. Roth
Adviser

Department of Physics

Dr. Connie B. Roth

Adviser

Dr. Stefan Boettcher

Committee Member

Dr. Tracy Morkin

Committee Member

2012

Effect of Thermal Conditions and Mechanical Stress During Vitrification on Physical Aging of Thin Polymer Films

By

Suk Whan Yoon

Dr. Connie B. Roth

Adviser

An abstract of
a thesis submitted to the Faculty of Emory College of Arts and Sciences
of Emory University in partial fulfillment
of the requirements of the degree of
Bachelor of Sciences with Honors

Department of Physics

2012

Abstract

Effect of Thermal Conditions and Mechanical Stress During Vitrification on Physical Aging of Thin Polymer Films

By Suk Whan Yoon

Glasses are formed by cooling, or quenching, a glass-forming material from above the glass transition temperature T_g to below T_g. Once formed, glasses undergo a process named physical aging to advance towards a stable equilibrium state because they are thermodynamically unstable. Thin glass-forming polymer films have previously exhibited inconsistent physical aging behaviors in that thin freestanding polysulfone (PSF) films 400 nm to 4000 nm thick have previously exhibited an increased aging rate with decreasing film thickness behavior while thin supported polystyrene (PS) films 100 nm to 2500 nm thick have previously exhibited no change in aging rate with decreasing film thickness. We resolve this inconsistency by showing that this difference arises because the PS and PSF films were prepared under different conditions. Various conditions that may affect the aging rate of thin polymer films are then examined. In particular, effects of mechanical stress during quenching and thermal conditions, such as annealing temperature, quench temperature, and quench rate through T_g were examined. It is shown that the aging rate of the thin film increases with respect to cooling rate at T_g, and that the quench temperature T_{quench} and annealing temperature do not affect the physical aging rate. The increased aging rate behavior of the film with increasing cooling rate was justified with a free volume and a potential energy landscape argument. Specifically, it was noted that a fast quench could trap glasses at a higher volume and energy state than a slow quench. Based on the suggestion that the potential energy landscape can be altered with stress and strain, we propose a possibility that stress during the thermal quenching process may trap glasses in a different energetic state, inducing a different aging behavior than would be expected of quenched films without stress. We hypothesize that, since thinner freestanding films – which undergo faster aging – experience a larger stress than thicker freestanding films, aging rate increases may correlate with applied stress, but more data must be collected before any conclusive relationship can be drawn between stress and physical aging rate.

Effect of Thermal Conditions and Mechanical Stress During Vitrification on Physical Aging of Thin Polymer Films

By

Suk Whan Yoon

Dr. Connie B. Roth

Adviser

A thesis submitted to the Faculty of Emory College of Arts and Sciences
of Emory University in partial fulfillment
of the requirements of the degree of
Bachelor of Sciences with Honors

Department of Physics

2012

Acknowledgements

I would like to thank Laura A. G. Gray for designing and constructing the heating chamber and the lever system with which most of my data were collected. Many thanks go out to Justin Pye for all his sincere help with the ellipsometer and the spin-coating techniques. Thanks to Emory University and the Petroleum Research Fund (Grant PRF-48927-DNI17) for providing funds for these experiments. Thanks to my advisor Dr. Connie B. Roth for her immense help in writing this thesis and for her many valuable lessons in the lab. Also thanks to the committee members, Dr. Morkin and Dr. Boettcher for their inputs.

TABLE OF CONTENTS

List of Figures

Figure 19. Semilog plot of normalized film thickness h/h_0 as a function of aging time for 980 ± 10 nm thick supported PS films quenched on different materials.

Figure 20. (a) Semilog plot of normalized film thickness h/h_0 as a function of aging time for 1400 ± 45 nm thick PS films supported on silicon demonstrating the effect of cooling rate on the physical aging rate. (b) Plot of the measured physical aging rate as a function of cooling rate (data and figures by Laura Gray from ref.[5]).

Figure 21. Illustration of excess volume generated with fast quench for a glassy material.

Figure 22. Behavior of polymer films under different thermal and mechanical conditions can be understood with a potential energy landscape picture. (a) Potential energy landscape as described by Stillinger[7] contains basins, or local energy minima, and transition states, or local energy maxima. (b) Lacks and Osborn[2] proposed that the potential energy landscape changes when stress or strain is applied to the glass.

Figure 23. Plot of normalized film thickness h/h_0 with respect to $\log_{10}$ of aging time for 1660 ± 30 nm thick PS films quenched freestanding under various stresses from weights placed onto the lever system.

Figure 24. Calculation of error for noisy aging data.

Figure 25. Normalized film thickness h/h_0 versus $\log_{10}$ of aging time for freestanding PS films 1660 ± 30 nm thick illustrating an anomalous aging behavior of the films stressed with a lever system.

Figure 26. Physical aging rate with respect to added weight for 1660 ± 30 nm freestanding PS films.

Figure 27. Picture of Teflon mass (0.0326g) hanging on a 1000 nm PS film.

Figure 28. Semilog plot of normalized film thickness h/h_0 as a function of aging time for 1000 ± 50 nm thick PS films quenched freestanding with a mass hung on the end.

INTRODUCTION

Polymers are long chains of molecules. Unlike small molecules that have great rotational and translational mobility, polymers have restricted motion that hinders their ability to pack quickly and efficiently into each other to form a crystal. If the hindrance to packing is great enough or if the shape of the molecule is irregular enough to prevent crystallization, polymers will not form crystals upon cooling but rather form glasses. Glasses are amorphous solids and are different from crystals in that they do not have a regular packing pattern; rather, microscopically, glasses appear like liquids, except the molecules are more or less locked in place in glasses[1]. Upon cooling, polymer liquids exhibit slower dynamics – such as slower flow rate or slower average molecular speeds – until it reaches a critical temperature, the glass transition temperature T_g, when the dynamics slow drastically to the point of near-complete arrest. Thus, depending on the cooling rate, the value of T_g may vary slightly. This transition is different from a first-order liquid to crystalline solid transition in that no discontinuous volume change occurs; however, the temperature-derivative of volume, or the slope of volume versus temperature graph, discontinuously changes to a lower value upon vitrification (refer to Figure 1a).

Polymer glasses are unstable because glasses are not at thermodynamic equilibrium at temperatures below their glass transition temperature: they have excess thermodynamic quantities such as volume, enthalpy, and entropy compared to equilibrium[2]. Because of the instability, polymer glasses relax towards the equilibrium state in a process named "physical aging," but this equilibrium state can only be attained in theory as the aging time approaches infinity. Physical aging leads to a more efficient packing of molecules and a corresponding decrease in the free volume, the free space available among the polymer molecules[2]. Physical

aging in glasses can be measured as a tiny decrease in overall volume and free volume, which corresponds to an increase in density and a decrease in gas permeability; it can also be measured as a slight increase in index of refraction. One can quantify the physical aging rate by monitoring the aforementioned physical parameters over the logarithm of time. On a logarithmic time scale these parameters age linearly, so the physical parameters can be fit to a line. The aging rate that one measures is in the "power law region" where the slope, $\partial V / \partial \log t_a$, is more or less constant (Figure 1b)[3]. Struik *et al.* defines the volumetric physical aging rate as follows[2]:

$$\beta_v = -\frac{1}{V_\infty}\frac{\partial V}{\partial \log t_a}$$

where β_v is the rate of volumetric physical aging, V_∞ is the theoretical equilibrium volume of polymer sample, and t_a is the aging duration. The partial derivative indicates that other factors that effect volume, such as temperature, are held constant.

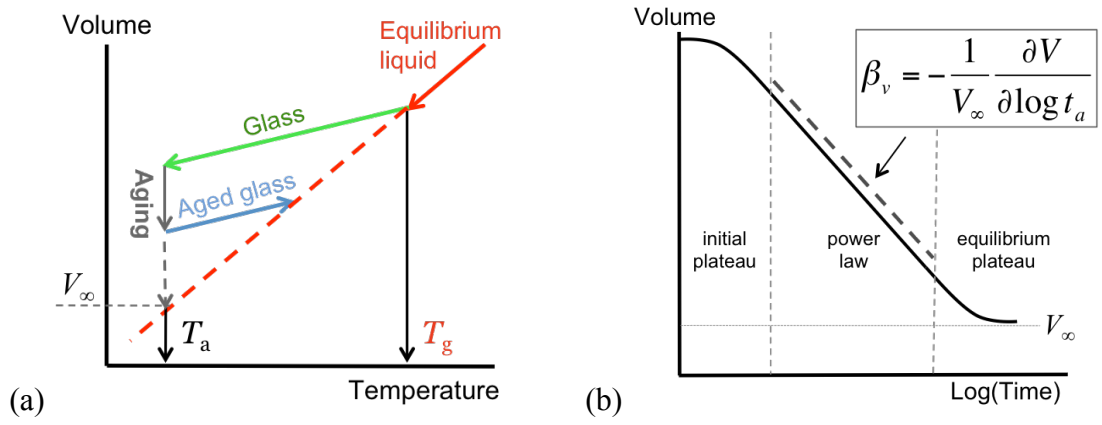

Figure 1. Schematic illustration of glass transition and physical aging. **(a)** When a glass-forming equilibrium liquid above T_g is cooled, the slope of volume versus temperature undergoes a discontinuous transition. Isothermal aging at T_a, the aging temperature, causes volume to decrease towards the dashed equilibrium volume. Theoretical equilibrium V_∞ can only reached if the aging time is infinite. **(b)** Volume curve upon isothermal aging. The slope of the graph in the power law region gives $\partial V / \partial \log t$, which can be used to find the aging rate, β_v.

Motivation

Changes in physical properties due to physical aging are often miniscule: for example, volume reduction from aging is on the order of 1% or less. However, from engineering perspective, even this small instability can render polymer glasses undesirable for industrial uses. Moreover, some physical properties such as gas permeability are more heavily affected by aging. Polysulfone (PSF) is a polymer that has favorable permeability and selectivity due to its high free volume and thus is used industrially as gas separation membrane[4]. In a study of gas permeability through a membrane of bulk (above ~4 μm thick) films and thin (0.4 - 4 μm thick) PSF gas separation membranes, Huang and Paul observed that oxygen permeability through the membrane decreased by 50-70% due to aging alone. More significantly, they have noted that thinner films undergo a faster decrease in permeability than thicker films for films 400 - 4 μm thick (Figure 2). Since membrane-based gas separation uses gas separation layers that are even thinner (<100nm)[5], it is crucial to search for a way to control physical aging in polymers with high free volume. Huang and Paul later monitored the index of refraction of PSF and other high free-volume polymers[6] with an optical technique termed ellipsometry, described in detail below, and observed that the optical properties of thinner PSF films also aged faster than thicker PSF films, as was suggested by their gas permeation studies[4]. The goal of this thesis will be to address the fundamental cause of this faster physical aging behavior in thinner films.

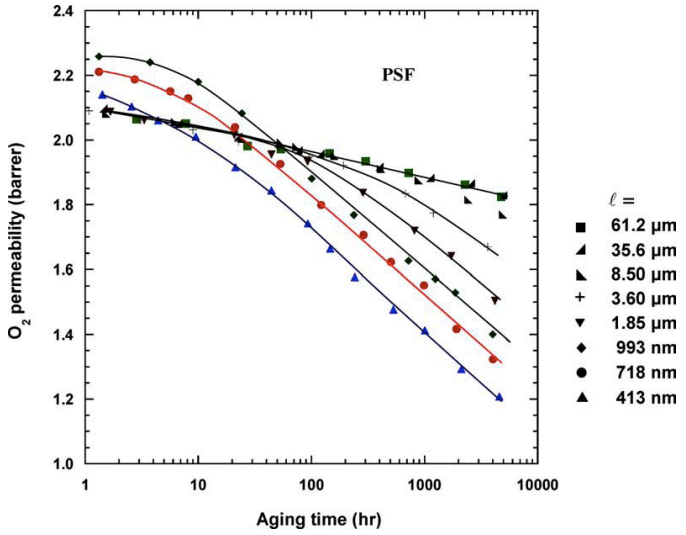

Figure 2. Semilog plot of oxygen permeability of PSF aged at 35°C as a function of aging time in hours. The decrease in oxygen permeability due to aging gets larger for thinner films (Reprinted with permission from ref. 4).

BACKGROUND

Ellipsometry

Ellipsometry is one of the most precise methods of measuring film thickness and optical properties of materials. Generally, in ellipsometry, a beam of light with a known polarization is passed through or reflected off of a sample, upon which the polarization is slightly altered. The new polarization of the emerging light is then measured and compared with the polarization of the original beam of light to obtain the optical properties of the sample. An ellipsometer is a device used to perform these necessary ellipsometric measurements. The author uses a model M-2000 variable angle spectroscopic ellipsometer (VASE) from J.A. Woollam Co. Inc., courtesy of

the Emory University Roth Lab under Dr. Connie Roth in which the author worked on this thesis.

The optical components used in an ellipsometer are a stable light source (Ls), polarizer (P), compensator (C, or Q for quarter-wave plate), optical system (sample) under study (S), analyzer (A) (another polarizer), and detector (D)[7]; the light generated by the light source travels through the components in the order listed (see Figure 3, next page). The light source used in our M-2000 ellipsometer is a tungsten lamp, which covers the wavelength range 300 - 1000 nm in which our ellipsometric measurements are done. The light is directed from the source towards the polarizer, which makes the light linearly polarized. The electric field of polarized light can be separated into two components: s-component, which is perpendicular to both the direction of propagation and the plane of incidence (or parallel to the plane of the film sample), and p-component, which is perpendicular to the direction of propagation but parallel to the plane of incidence. As the linearly polarized light passes through the compensator, which is a quarter-wave plate, one of the two components is retarded by quarter of a wavelength, equivalent of a 90° phase shift. This makes the light elliptically polarized. The light beam is then reflected off of a sample, upon which the polarization changes. An analyzer – essentially another polarizer – is used to analyze the emerging elliptically polarized light. A charge-coupled device (CCD) array is used as the detector to measure the entire spectrum at once.

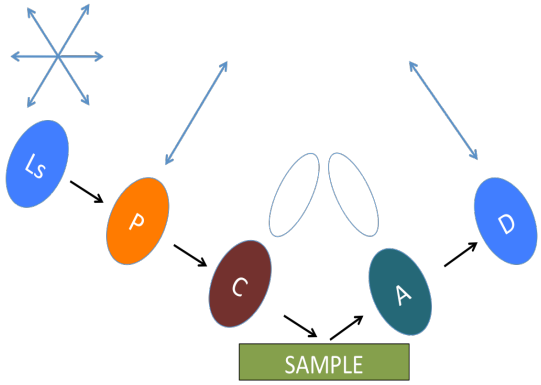

Figure 3. A schematic of the optical components used in a typical ellipsometer. An unpolarized beam of light generated by the light source (Ls) passes through a polarizer (P) then is elliptically polarized with a compensator (C). The beam of light then reflects off of the sample, which in our case is a polymer film supported on silicon. Polarization and intensity of light changes upon reflection, and these changes are measured with an analyzer (A) and then a detector (D).

The parameters calculated from the spectrum are the ellipsometric angles Ψ and Δ, where $\frac{R_{total,p}}{R_{total,s}} \equiv \tan\Psi \cdot e^{i\Delta}$. $R_{total,s}$ and $R_{total,p}$ are the complex ratios of electric field amplitudes of the light ray that reflects off of the sample to that of the incident light ray for s- and p-components, respectively. To understand the significance of these parameters one needs to be familiar with concepts of thin film interference. A schematic structure of the sample is shown in Figure 5 in page 8. The material of interest is the polymer layer, which is supported on a substrate; we use a silicon wafer as our substrate because the optical properties of silicon are well defined. When incident light reaches a surface some of it is reflected and some of it is transmitted; the s- and p-components reflect and transmit differently from each other upon reaching the surface. The amplitudes of the electric fields of the reflected and transmitted light, E_r and E_t, can be calculated from the Fresnel coefficients, r_s, r_p, t_s, and t_p[8]:

$$r_s \equiv \left(\frac{E_r}{E_0}\right)_s = \frac{n_i\cos\theta_i - n_t\cos\theta_t}{n_i\cos\theta_i + n_t\cos\theta_t} \qquad r_p \equiv \left(\frac{E_r}{E_0}\right)_p = \frac{n_t\cos\theta_i - n_i\cos\theta_t}{n_i\cos\theta_t + n_t\cos\theta_i}$$

$$t_s \equiv \left(\frac{E_t}{E_0}\right)_s = \frac{2n_i\cos\theta_i}{n_i\cos\theta_i + n_t\cos\theta_t} \qquad t_p \equiv \left(\frac{E_t}{E_0}\right)_p = \frac{2n_i\cos\theta_t}{n_i\cos\theta_t + n_t\cos\theta_i}$$

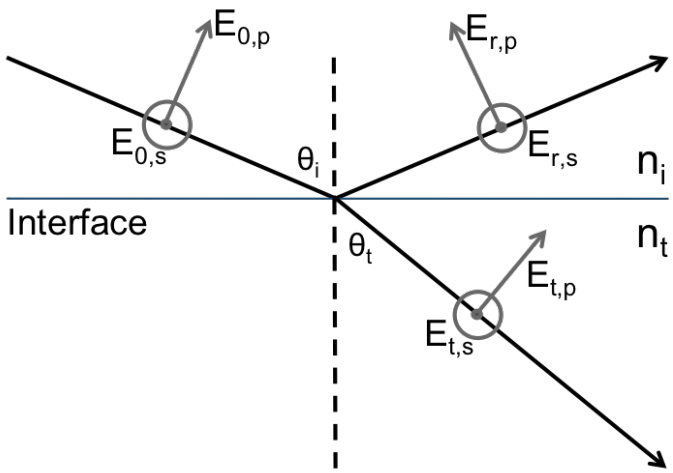

Figure 4. Supplementary figure for understanding the variables in calculation of the Fresnel Coefficients. Light with electric field amplitude components $E_{0,s}$ and $E_{0,p}$ incident on a surface will be both transmitted and reflected. Transmitted light will have amplitude $E_{t,s}$ or $E_{t,p}$ equal to $t_sE_{0,s}$ or $t_pE_{0,p}$; reflected light will have amplitude $E_{r,s}$ or $E_{r,p}$ equal to $r_sE_{0,s}$ or $r_pE_{0,p}$.

where E_0 is the amplitude of the electric field of the incident light, r_s and r_p are Fresnel reflection coefficients, t_s and t_p are Fresnel transmission coefficients, n_i and n_t are indices of refraction, and θ_i and θ_t are incident and transmitted angles. The subscripts s and p represent the s-component and p-component of light, and the subscripts i and t represent incident and transmitted light. Refer to supplementary Figure 4 for visualization of these variables.

Refer to Figure 5 to help visualize the following section. When elliptically polarized light reaches the air-polymer surface, reflected light is directed towards the detector while transmitted light continues towards the polymer-silicon surface. Reflection occurs again at the polymer-silicon surface, and light travels back towards the air-polymer surface where some of it is transmitted and some of it is reflected back towards the polymer-silicon surface. This process continues semi-infinitely, and the resultant reflected light from the sample is approximately the infinite sum of all of these emerging rays of light. The first ray that is reflected off of the air-

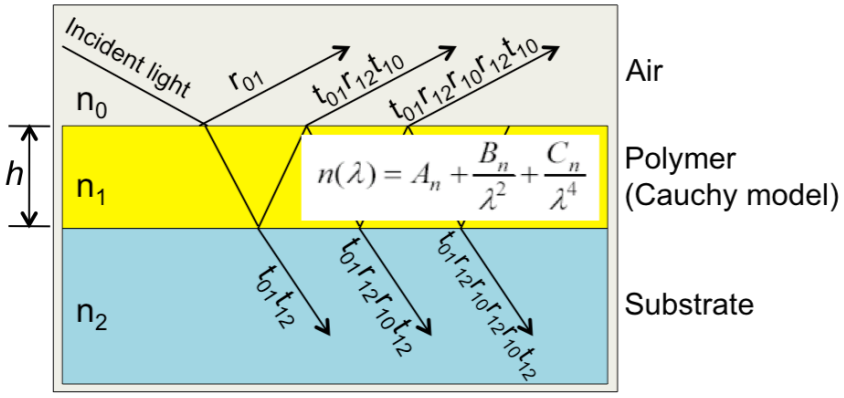

Figure 5. A schematic of the sample. Typically, the substrate is silicon. A computer is used to fit the measured data with the Cauchy model to calculate the index of refraction and thickness *h* for the polymer layer. Some incident light from the air is reflected and some is transmitted upon reaching the polymer-air interface. The transmitted light heads toward the polymer-substrate interface, where again some light is reflected and some light is transmitted.

polymer surface has electric field amplitude E_0r_{01} (subscript "01" for air-polymer surface). The first ray that emerges from within the film has amplitude $E_0t_{01}r_{12}t_{10}$ (subscript "12" for polymer-silicon surface), but with a different phase compared to the reflected ray because the emerging ray traveled an extra distance through the polymer film before it emerged. Note that t_{01} and t_{10} are two different quantities: subscript "01" means passing from air to polymer while subscript "10" means passing from polymer to air. The phase difference can be accounted for by multiplying the second electric field by $e^{-2i\beta}$, where $\beta = 2\pi\left(\frac{h}{\lambda}\right)n\cos\theta_r$ is the phase shift, assuming air has n_0=1. The addition of the electric fields of all of the rays is then:

$$E_{total} = E_0(r_{01} + t_{01}t_{10}r_{12}e^{i2\beta} + t_{01}t_{10}r_{10}r_{12}^{\ 2}e^{i4\beta} + t_{01}t_{10}r_{10}^{\ 2}r_{12}^{\ 3}e^{i6\beta} + ...) = E_0R_{total}$$

Given that $-r_{01} = r_{10}$ and $t_{01}t_{10} = 1 - r_{01}^{\ 2}$:

$$R_{total} = r_{01} + (1 - r_{01}^{\ 2})r_{12}e^{i2\beta} \cdot \sum_{n=0}^{\infty}(-r_{01}r_{12}e^{i2\beta})^n$$

The geometric series converges: $\sum_{n=0}^{\infty}(-r_{01}r_{12}e^{i2\beta})^n = \frac{1}{1+r_{01}r_{12}e^{i2\beta}}$. Thus, the above equation reduces to:

$$R_{total,s} = \frac{r_{01,s} + r_{12,s}e^{i2\beta}}{1 + r_{01,s}r_{12,s}e^{i2\beta}} \text{ (for s-component)}$$

$$R_{total,p} = \frac{r_{01,p} + r_{12,p}e^{i2\beta}}{1 + r_{01,p}r_{12,p}e^{i2\beta}} \text{(for p-component).}$$

Note that R_{total} is a complex number that accounts for both the amplitude and the phase of the electric fields. This brings us back to the definition of ellipsometric angles Ψ and Δ. In ellipsometry, by definition:

$$\frac{R_{total,p}}{R_{total,s}} \equiv \tan\Psi \cdot e^{i\Delta}$$

Ψ and Δ are functions of wavelength λ and are measured directly from the spectrum. Tan Ψ is the ratio of the total reflectance of the p-component to that of the s-component, and Δ is the change in phase difference between the two components upon reflection off of the sample. Given an index of refraction model for the polymer layer and the silicon substrate, the computer can generate Ψ(λ) and Δ(λ) to fit to the measured data.

The model used for the polymer layer is a Cauchy model for transparent materials, which expresses index of refraction as a function of wavelength of light[7]:

$$n(\lambda) = A + \frac{B}{\lambda^2} + \frac{C}{\lambda^4} + ...$$

where A, B, and C are arbitrary constants with λ traditionally taken to be in micrometers (μm). This model provides a great approximation for index of refraction of transparent materials for 400 - 1000 nm wavelength range. The silicon substrate is well defined: on its surface there is 2 nm-thick layer of SiO_2 with a known index of refraction n~1.56, and a silicon layer underneath

with n~3.8. Tabulated values from the literature are used by the computer for n(λ) of SiO_2 and Si. With these models the computer can now calculate $R_{total,p}$ and $R_{total,s}$ by varying the thickness of the polymer layer and the index of refraction (by varying parameters A, B, and C of the Cauchy layer). Using the definition of Ψ and Δ above, the computer can generate Ψ and Δ from R_{total} to fit with the experimental data. The fit is done using a least-squares minimization.

Existing Literature

Using ellipsometry, Huang and Paul[6] monitored index of refraction of high free volume polysulfone (PSF) films over a period of 10000 hours (little over a year). PSF has a high free volume due to its rigid chemical backbone, the main chain of a polymer. The aromatic groups and electron lone pairs on the ether group hinder flexible movement of the backbone (Figure 6), increasing the amount of free volume among the polymers, just as a ball of flexible yarn packs better than a ball of stiff iron strings. High free volume polymers exhibit high permeability and selectivity, so they are frequently subjects of interest in membrane-based gas permeation studies. Huang and Paul performed a series of experiments to characterize physical aging of high free volume polymers frequently used in gas permeation[6]. The sample preparation procedure involved a "freestanding quench" used to mimic the preparation procedures used for the gas

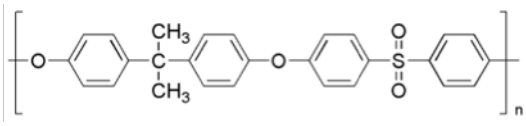

Figure 6. Chemical structure of polysulfone (PSF), a stiff backbone polymer.

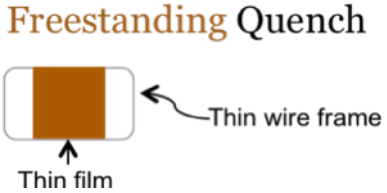

Figure 7. A schematic of a freestanding quench sample. A film is draped across the width of a thin steel wire frame.

permeation studies. The freestanding quench involved cooling (quenching) of polymer films from the liquid state to glassy state (through T_g) as they hang on a thin wire frame, described in Figure 7. Quenching initiates physical aging. The films were then transferred onto a silicon substrate for ellipsometric measurements of the index of refraction every few days. In between measurements, the films were stored at the aging temperature, typically 35°C. Huang and Paul observed that for films with thickness 400 nm to 1000 nm, thinner films age faster than thicker films (Figure 8). Note that the index of refraction *increases* as aging progresses; thus, steeper slope indicates higher physical aging rate. It is noteworthy that in the same paper it was shown that films of other high free volume polymers such as Matrimid® 5128 (a polyimide) and poly(2,6-dimethyl-1,4-phenylene oxide) (PPO) were also shown to exhibit accelerated (faster) aging rates with decreasing film thickness.

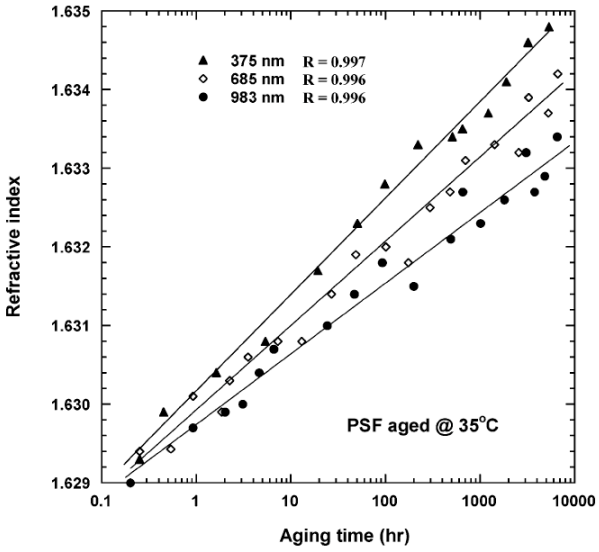

Figure 8. Semilog plot of refractive index as a function of aging time in hours for PSF quenched freestanding. The slope of the lines represents the aging rate. It can be seen that the 375 nm thick PSF film (closed triangles) ages faster than the 685 nm thick PSF films (open diamonds), and that 685 nm thick PSF films age faster than the 983 nm thick PSF films (closed circle), indicating that aging increases with film thickness (Reprinted with permission from ref. 6).

Huang and Paul's research was painstakingly lengthy – the measurements themselves took over 10000 hours to complete. Baker *et al.*[9] under Emory University's Roth Lab has developed a streamlined ellipsometric procedure that reduced the time required to reliably measure the aging rate to 6 hours. In addition, a modified method of determining the aging rate using the thickness of polymer film h was evaluated. Baker *et al.* defines the aging rate as,

$$\beta \approx -\frac{1}{h_0}\frac{\partial h}{\partial \log t_a}$$

where β is the aging rate, h_0 is the polymer film thickness after 10 minutes of aging, and t_a is the aging duration. With this equation one can simply graph h/h_0 over $\log t_a$ and measure the slope of the line to determine the aging rate.

The equation is a straightforward modification from Struik's original definition of aging rate[2]:

$$\beta_v = -\frac{1}{V_\infty}\frac{\partial V}{\partial \log t_a}$$

The polymer film is restricted to a substrate with fixed area, so the volume of the polymer film V (=area × h) is directly proportional to h. Thus V/V_∞= (area × h) / (area × h_∞) = h/h_∞. The equilibrium height of the film h_∞ is approximately equal to h_0 since the volume decrease due to aging is only on the order of 1% or less. Baker *et al.* demonstrated that replacing h_∞ by h_0 has an inconsequential effect on the value of the aging rate.

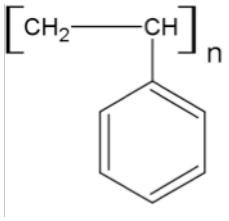

Figure 9. Chemical structure of polystyrene (PS), a flexible C-C backbone polymer.

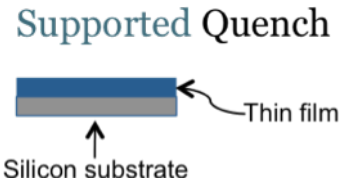

Figure 10. A schematic of a supported quench sample. A polymer film is cooled as it is resting on a silicon substrate.

With this procedure developed by Baker *et al.*, Pye *et al.*[10] under Emory University's Roth Lab investigated the physical aging of thin polystyrene (PS) films at various film thicknesses. PS is a common polymer with a flexible C-C backbone and bulky phenyl side groups that limit its packing in the glassy state (Figure 9). In this study, Pye et al. prepared the films for aging measurements with a "supported quench." A supported quench involves cooling polymer films from liquid state to glassy state *as they rest on the silicon substrate* (Figure 10). As can be seen from Figure 11 below, for the film thickness range of 100 nm to 2500 nm, the physical aging rate is independent of film thickness, unlike Huang and Paul who observed an increase in aging rate for PSF films of 400 nm to 1000 nm thick as film thickness decreased. The decrease in the aging rate for ultrathin films (<100 nm thick) is due to free surface effects that only affect a small portion of the film near the free surface and is inconsequential for the thicker films studied in my thesis.

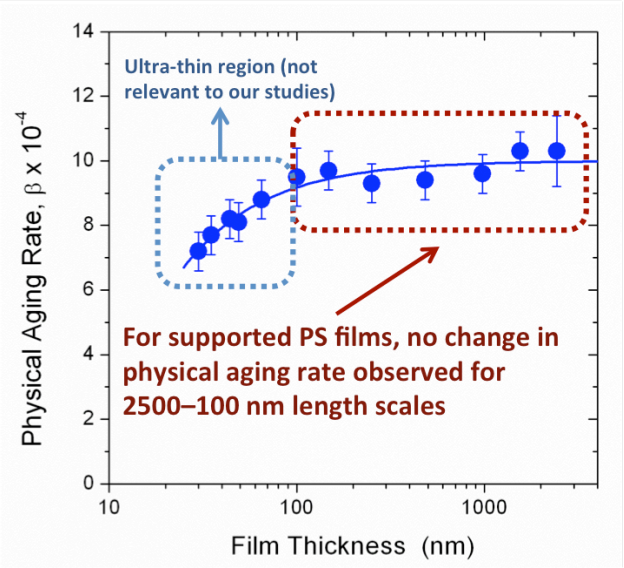

Figure 11. Physical aging rate as a function of film thickness for PS films quenched supported, aged at 65°C. It can be seen that the aging rate for films above 100 nm does not depend on the thickness of the film (Figure adapted with permission from Pye *et al.*, ref. 10).

In related research, Gray *et al.*[11] under our Emory University Roth Lab directly compared the aging behavior of PS films quenched in a freestanding state to that of PS films quenched in a supported state. The purpose was to determine if quench conditions during glassification of a polymer liquid affect the physical aging rate. Figures 12a and 12b each show physical aging data of polystyrene when quenched freestanding (circles, higher line) and when quenched supported (triangles, lower line) for 1260 nm (a) and 600 nm (b) thick PS films. The β aging rates of 1260 nm and 600 nm thick films quenched supported were 9.5 x 10^{-4} and 9.3 x 10^{-4}, respectively, while those quenched freestanding were 6.0 x 10^{-4} and 8.1 x 10^{-4}. As we can see, the freestanding PS films show accelerated (faster) physical aging rate with decreasing thickness, as did the freestanding PSF films in Huang and Paul's experiments.

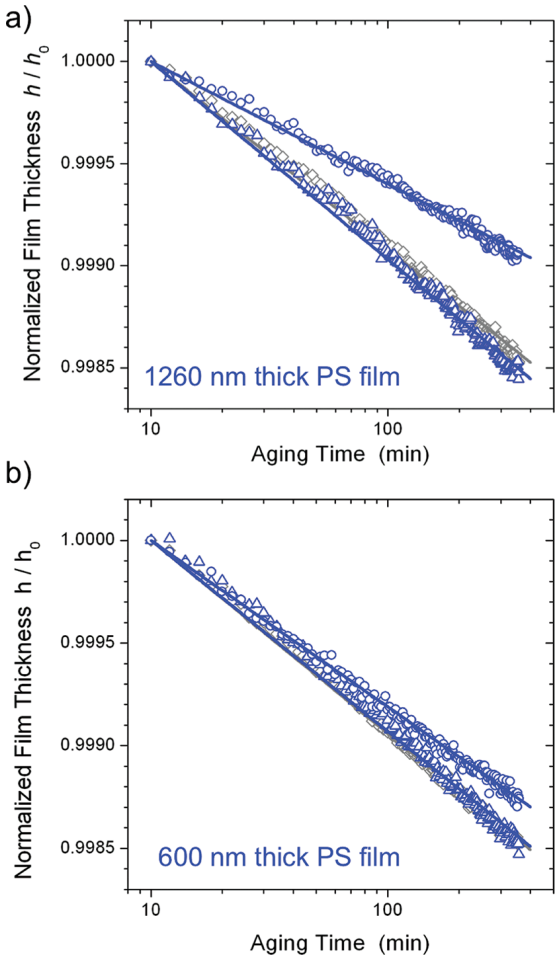

Figure 12. Semilog plot of normalized film thickness h/h_0 versus aging time. Each graph shows three physical aging data sets – circles, gray diamonds, and triangles – for a) 1260 nm thick PS films and b) 600 nm thick PS films using the technique developed by Baker *et al.* Blue circles (higher line) represent films annealed above T_g until equilibrium is attained then quenched freestanding. Gray diamonds represent films equilibrated then quenched supported. Blue triangles (lower line) represent the films initially quenched freestanding, but equilibrated a second time above T_g before being quenched supported. The β aging rates of 1260 nm and 600 nm thick films quenched supported were 9.5×10^{-4} and 9.3×10^{-4}, respectively, while those quenched freestanding were 6.0×10^{-4} and 8.1×10^{-4} (Reprinted from Gray *et al.*, ref. 11)

OPEN QUESTIONS AND GOALS OF THIS THESIS

The literature on physical aging of polymer films as it stands now presents some contradictions. For example, films of PSF – and other stiff-backbone polymers –400 nm to 1000 nm thick prepared freestanding have previously exhibited accelerated aging with decreasing thickness, as in the paper by Huang and Paul[6]. However, Pye *et al.*[10] demonstrated that flexible-

backbone PS films with thickness ranging from 100 to 2500 nm prepared supported age at the same rate. Then there is Gray *et al*.[11] that demonstrates that 600 nm - thick PS film exhibits higher physical aging than 1200 nm - thick PS film when they are prepared freestanding. The main source of the confusion is the fact that there are two variables that might affect the physical aging rate in the literature: chemical stiffness and quenching method. We must separate out the variables in order to clearly see what is causing the accelerated aging behavior.

Stiff Backbone vs. Flexible Backbone Polymers

Gray *et al*.[11] already attempted to separate the variables by testing supported and freestanding films made out of a single material, the flexible backbone polymer PS. As explained before, the paper shows that supported PS films exhibit no increasing aging rate with decreasing thickness behavior while freestanding PS films exhibit such behavior. This strongly suggests quench conditions, rather than the chemical identity of the polymer glass, is responsible for this accelerated aging behavior. *An experiment that would strengthen this argument would be physical aging data for PSF supported films at different thicknesses*: if thinner PSF films do not exhibit higher aging rate, then this would decisively rule chemical stiffness out as the cause of the accelerated aging rate behavior.

Freestanding vs. Supported Quenching Method

If stiffness is ruled out, this leaves quench method as the possible cause. If quench method is indeed the cause of this accelerated aging, what is the fundamental difference between the two quenching methods, supported and freestanding, that might be causing this behavior? Specifically, *what physical parameters may also be increasing or decreasing with decreasing*

film thickness for freestanding films but kept constant in supported films as they are quenched?

I have addressed the questions above in this thesis by first observing the aging behavior of PSF films of thicknesses 400nm and 1000nm prepared supported, then investigating different quenching conditions that may affect the physical aging rate of freestanding and supported PS films. Specifically, I varied the *annealing* and *quench temperature* (the temperature to which films are quenched from above T_g), the *cooling rate* during vitrification, and the *stress* on the film during vitrification. Cooling rate and stress on the film are constant for supported films but increasing with decreasing thickness for freestanding films, so they might be the physical parameters responsible for the difference between the physical aging rates of supported films and those of freestanding films.

EXPERIMENTAL PROCEDURES

Sample Preparation

Polystyrene (PS), M_n = 132 kg/mol, M_w = 289 kg/mol, and polysulfone (PSF), M_n = 26.9 kg/mol, M_w = 67.5 kg/mol, were purchased from Scientific Polymer Products. Films were made by dissolving PS in toluene or PSF in cyclopentanone, and then spin coating the solutions onto freshly cleaved 1 in. × 2 in. mica for freestanding films or 1 in. × 1 in. silicon wafers with native oxide coatings (SiO_2) for supported films. Spin coating is a technique in which polymer solutions are dropped onto the substrate then spun. The concentration of the solution used and the spin

speed determines the thickness of the polymer film[12]. The spun films were subsequently annealed for at least 12 h under vacuum at 120°C for PS (20°C above T_g of PS, ~100°C), or 150°C for PSF (35°C below T_g of PSF, ~185°C, but the same annealing temperature used by Huang and Paul[6]), in order to remove any solvent from the films. PS films spun on mica were cut with a surgical knife so that its width is 1.00 cm wide. The film was then separated from its mica substrate, done by gently dipping the mica with film in water. The PS film floating on water was caught so that the two ends of the film are in contact with a specially designed sample holder (shown in Figure 13b, next page). After the film was dried for 30 minutes, the sample holder was transferred to a lever system to prepare for freestanding quench under stress. The lever system is arranged so that a weight hung on the other side of the fulcrum applies stress to the freestanding film during quenching. A schematic of the set-up is illustrated in Figure 13a. The two lever arm lengths, d_1 and d_2, were measured to be 46.37 mm and 101.25 mm, respectively. Two pins are inserted below the fulcrum to keep the stress from being applied to the film during annealing. The freestanding film is then enclosed in a well-insulated heating chamber.

All films, supported or freestanding, were annealed above T_g for 30 min, typically at 120°C for PS or 215°C for PSF. The supported films were then quenched to a temperature T_{quench}, typically room temperature unless otherwise noted, by quickly removing the films from the oven and placing them in contact with a large thermal mass (an aluminum block, unless otherwise stated) equilibrated to T_{quench}. Quenching initiates the physical aging process in the films. For the freestanding films, during the last minute of annealing, the pins that kept the stress from the weight from being applied were taken out. This is to make sure the film is at mechanical equilibrium with the given stress. To quench the film, the cover of the insulated chamber was

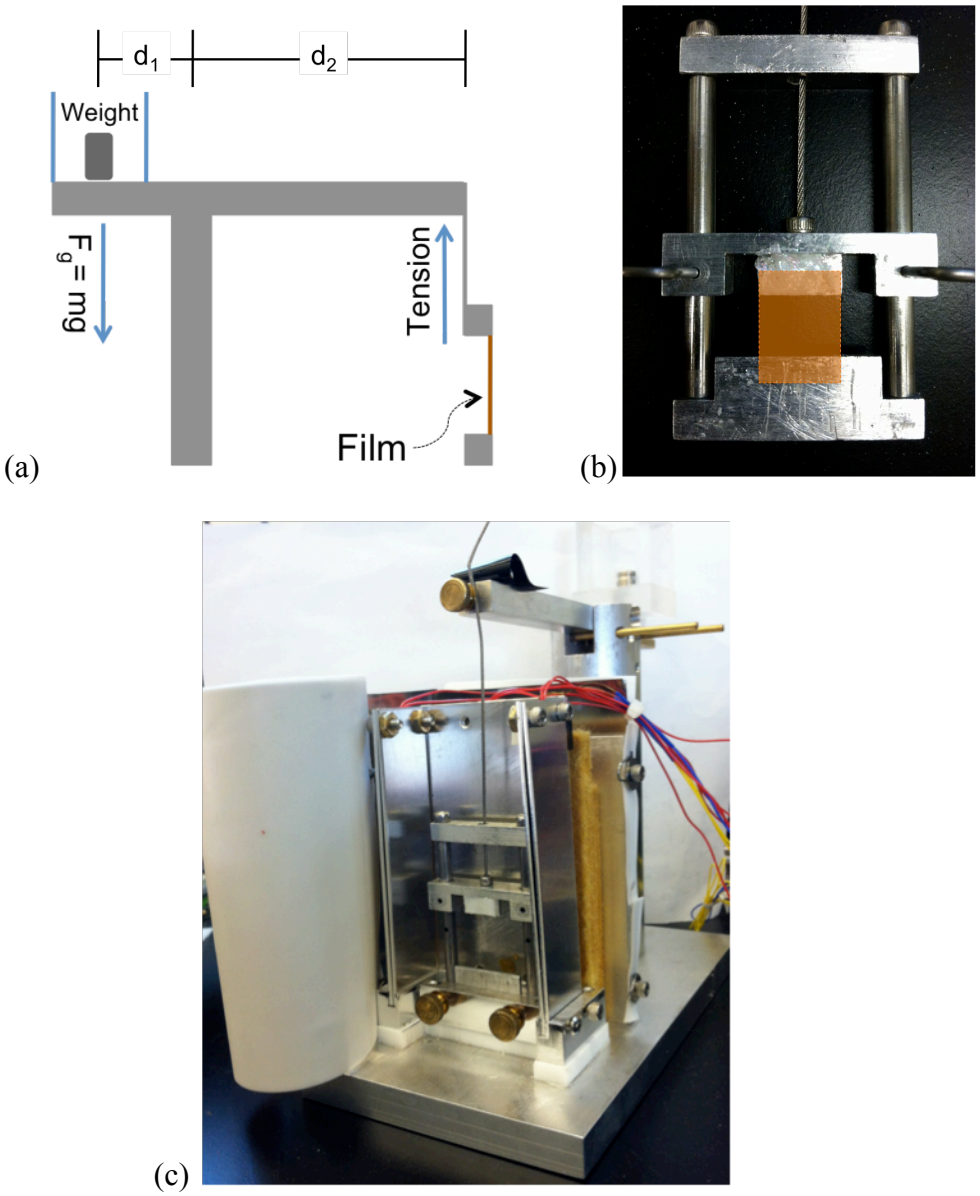

Figure 13. (a) Schematic of the lever system used to apply stress to a freestanding film. (b) Picture of the specially designed sample holder. The polymer film is draped across the shaded part of the sample holder, and the steel wire is connected to the lever system so that the tension on the wire applies stress to the film. After quenching, the film is transferred onto silicon for ellipsometric measurements. (c) Picture of the experimental set-up. The chamber within which the sample holder is held is heated up to the annealing temperature, 120^{o}C. The chamber is closed with a Teflon cover then sealed up with aluminum foil placed on top. A weight is placed in the transparent weight holder (visible on top right corner). Two gold-colored pins keep the weight from applying a stress to a film. To apply a stress, the back pin is pulled out.

opened for 1 minute to let room temperature air enter the chamber. Once quenched, the freestanding films were then transferred to silicon wafers for the physical aging measurements with ellipsometry. Since the lever system is designed to be balanced when no additional weight *m* is added, stress σ on the film can be determined by calculating the tension on the film, $Tension = mgd_1/d_2$ (where *m* is mass in kg of the weight and g is gravity, 9.81 m/s^2), then dividing the tension by cross sectional area of the film, $A = hw$, where *h* is the thickness and w is the width (1.00 cm) of the film: $\sigma = Tension/hw = mgd_1/hwd_2$.

Supported films were already prepared on silicon, so no transfer was necessary. Thicknesses of the films were monitored by ellipsometry during the aging process for 3 - 12 hours. It is important to note that freestanding films thicken upon annealing above T_g. This behavior has been observed in Gray *et al.*[11] and Huang and Paul[6]. In both papers, the reported film thicknesses are the post-annealed film thicknesses, before aging measurements. The same shall be the case for freestanding film thicknesses reported in this thesis. Most of the freestanding films used for experiments involving mechanical stress were aimed to be 1500 nm thick before annealing. After annealing they thickened to around 1660 ± 30 nm, although a few of the films thickened to 1800 nm.

Aging Measurements by Ellipsometry

Immediately after quenching, the samples were placed on the ellipsometer hot stage (Instec HCS 302) that was pre-equilibrated at the aging temperature T_a, typically 65^{o}C for PS and 100^{o}C for PSF unless otherwise noted. Using spectroscopic ellipsometry with the J. A. Woollam M-2000, the theory and instrumental setup of which are described in the Ellipsometry backgrounds subsection, the film thickness was monitored over time. Following the procedure

developed in our lab in Baker *et al.*[9] (refer to Background section), the ellipsometric angles $\Psi(\lambda)$ and $\Delta(\lambda)$ were collected every 2 minutes, averaging over a period of 30 s, throughout the aging measurement lasting several hours. The film thickness h and index of refraction $n(\lambda)$ were determined by fitting $\Psi(\lambda)$ and $\Delta(\lambda)$, for λ = 400 - 1000 nm. The sample was modeled as a polymer film approximated as a Cauchy layer with $n(\lambda) = A + B/\lambda^2 + C/\lambda^4$ [7] with a 2 nm thick native oxide (SiO_2) layer underneath. As in Baker *et al.*, the physical aging rate β was determined by measuring the slope of the normalized film thickness h / h_0 graphed as a function of the logarithm of the aging time: $\beta = -1/h_0 \, dh / d(\log t)$, where h_0 corresponds to the film thickness at an aging time of 10 minutes. To minimize sample exposure to oxygen at high temperature, dry nitrogen gas (≥99.999% purity) was continuously flowed through the sample chamber for aging runs above 80°C. Figure 14 shows the heating protocol followed by all polymer films over the course of sample preparation for the physical aging measurements.

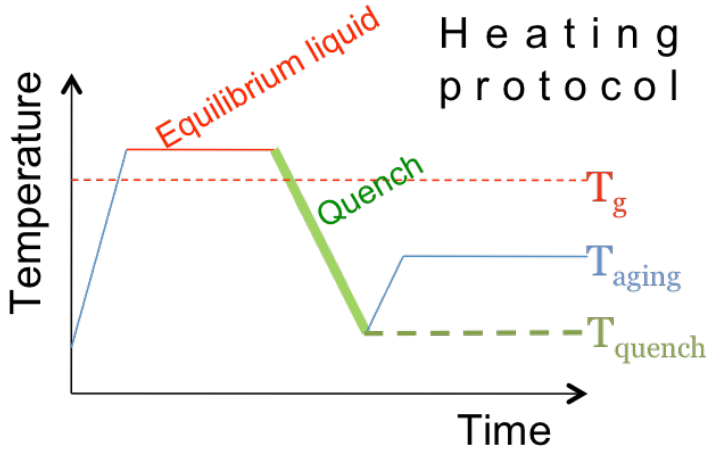

Figure 14. Heating protocol followed to prepare a film for aging measurements. A film is first annealed (or equilibrated) above T_g for 30 minutes to erase all thermal history before it is quenched below T_g to T_{quench}. The film is then heated up to T_{aging} for aging measurements.

RESULTS AND DISCUSSION

Chemical Structure: Stiff Backbone vs. Flexible Backbone

As explained in the Background section, the paper by Gray *et al.*[11] has demonstrated that PS freestanding films undergo accelerated aging with decreasing film thickness, while PS supported films exhibit constant aging rate with decreasing film thickness for the thickness range 100 – 2500 nm[10]. This suggested that the quenching method rather than chemical stiffness could be the cause of the accelerated aging with decreasing film thickness behavior. Data that would supplement this claim greatly is to examine the behavior of supported-quench films made from PSF, a chemically stiff polymer previously shown to age faster with decreasing thickness when prepared freestanding. If supported PSF films exhibit constant aging rate with decreasing film thickness, this would rule out chemical stiffness as the cause of the accelerated aging behavior. Figure 15 shows the result of 12-hour aging runs for PSF films that are 400±10 nm and 1000 ± 20 nm thick (three data sets for each thickness), aged at 100^{o}C. Nitrogen gas was run through the sample chamber to prevent air from degrading the PSF film. The aging temperature of 100^{o}C was chosen for PSF to be in the middle of the peak in aging rate[2]. I also tried an aging temperature of 35^{o}C to match that of Huang and Paul[6], but little aging was observed during the 12-hour period.

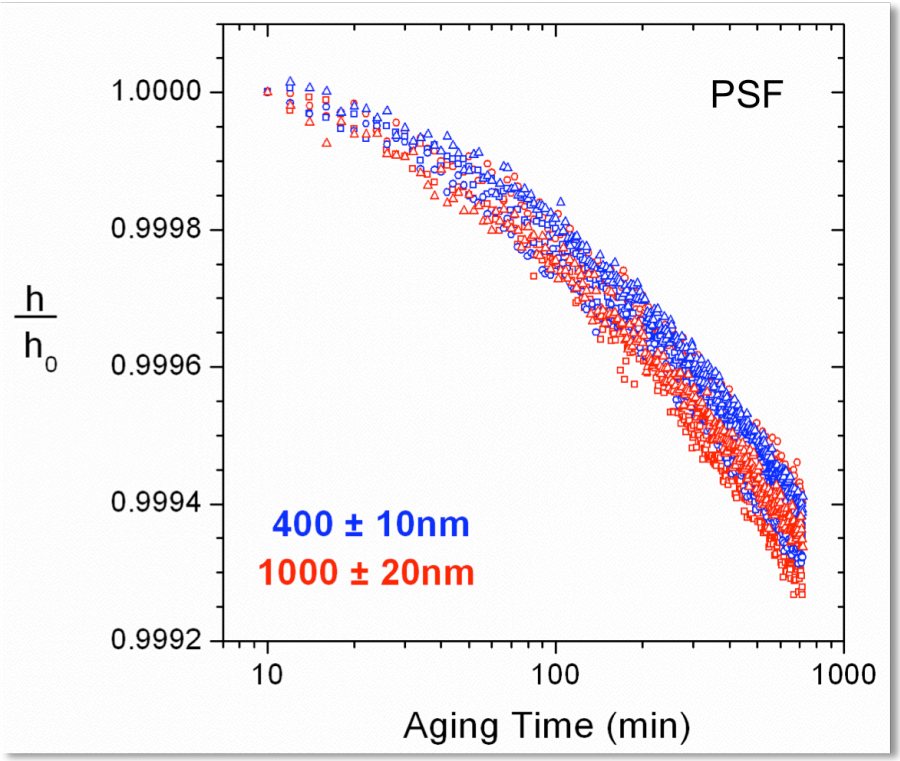

Figure 15. Semilog plot of normalized film thickness h/h_0 (normalized by thickness h_0 at 10 minutes) as a function of aging time for PSF films supported on silicon. The films were aged for 12 hours at 100°C. Blue data are PSF films 400 ± 10 nm thick films, and red data are PSF films 1000 ± 20 nm thick films. Three sets of data for each thickness is graphed here. Aging temperature of 100°C was used. All of these curves collapsed onto one curve, strongly indicating that the aging rates of supported PSF films are not thickness-dependent.

The plateau observed at the beginning of the aging run is due to the "initial plateau" effect[3] described in the Introduction section. Although the exact numerical values of aging rate were not determined due to the inflections in the plots, it can be observed that all six curves are equivalent to within the variability of the measurement. This is a strong indication that the aging rates of supported PSF films ~400 nm thick and films ~1000 nm thick are equal. Thus, we can conclude with high confidence that supported PSF films exhibit no accelerated aging behavior, and that quench method rather than chemical stiffness is the cause for accelerated aging observed in freestanding PSF films (by Huang and Paul[6], as explained in the Backgrounds section).

Quench Conditions: Annealing and Quench Temperatures

This leaves conditions during the quench as the likely cause for the accelerated aging behavior. To prepare a film, a set temperature protocol is followed: first annealing above T_g, followed by quenching to T_{quench}, then heating up to the aging temperature (typically 65°C for PS films found to be the peak in aging rate by Baker *et al.*[9]) for aging measurement. Refer back to the heating protocol, Figure 14 in the Experimental Procedure section, as needed. I tested if the annealing conditions above T_g have any effect on the physical aging rate by changing the

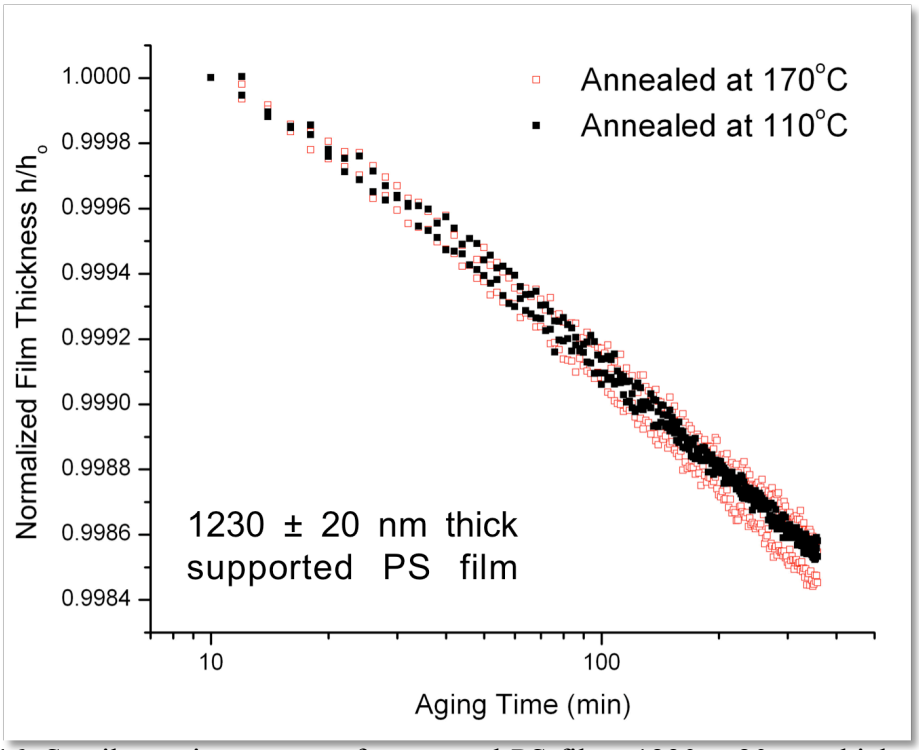

Figure 16. Semilog aging curves of supported PS films 1230 ± 20 nm thick annealed at 110°C (black, closed squares) or 170°C (red, open squares) before quenching for aging measurement. The films were aged for 6 hours at 65°C. Two data sets are shown for each annealing condition. The annealing conditions seem to have little to no effect on the aging rate of the films. The aging rate for the films annealed at 110°C for 25 min was $\beta = (9.2 \pm 0.6) \times 10^{-4}$, and that for the films annealed at 170°C for 25 min was $\beta = (9.3 \pm 0.6) \times 10^{-4}$.

annealing temperature to 110°C (~10°C above the T_g for PS) and 170°C for supported films 1230 ± 20 nm thick (Figure 16) before quenching to the room temperature for 6-hour aging runs at

65°C. Because PS supported films are easier to prepare than PS freestanding films, supported films were used to perform these experiments. The aging rate for the films annealed at 110°C for 25 min was $\beta = (9.2 \pm 0.6) \times 10^{-4}$, and that for the films annealed at 170°C for 25 min was $\beta = (9.3 \pm 0.6) \times 10^{-4}$. These values match well with the aging rate for the films under standard annealing condition of 20 min at 120°C, $\beta = (9.7 \pm 0.6) \times 10^{-4}$, strongly suggesting that varying annealing conditions above T_g do not affect the measured physical aging rates of the films. This is an intuitive result, as annealing above T_g erases prior thermal history and brings the films to thermodynamic equilibrium.

It is known that the aging temperature affects aging rate[9]; thus, it is always kept constant at 65°C. Variations in *quench* temperature, T_{quench}, and its influence on aging rate have not been studied extensively before. In order to study the effect of quench temperature on physical aging, I made a set of 1250 ± 10 nm thick PS supported films and varied the quench temperature to 25°C, 45°C, and 65°C by placing the annealed (thus equilibrated) films onto a large thermal mass at T_{quench}. The results of 6-hour aging runs are shown in Figure 17. Note that each curve is an overlap of two data sets, showing the high reproducibility of the results. A trend can be seen: a film exhibits a higher aging rate with decreasing quench temperature. Films quenched to 25°C, 45°C, and 65°C exhibited aging rates of $\beta = (9.1 \pm 0.2) \times 10^{-4}$, $(8.6 \pm 0.2) \times 10^{-4}$, and $(7.8 \pm 0.1) \times 10^{-4}$, respectively. This suggests that the thermal cooling process is an important factor that affects physical aging.

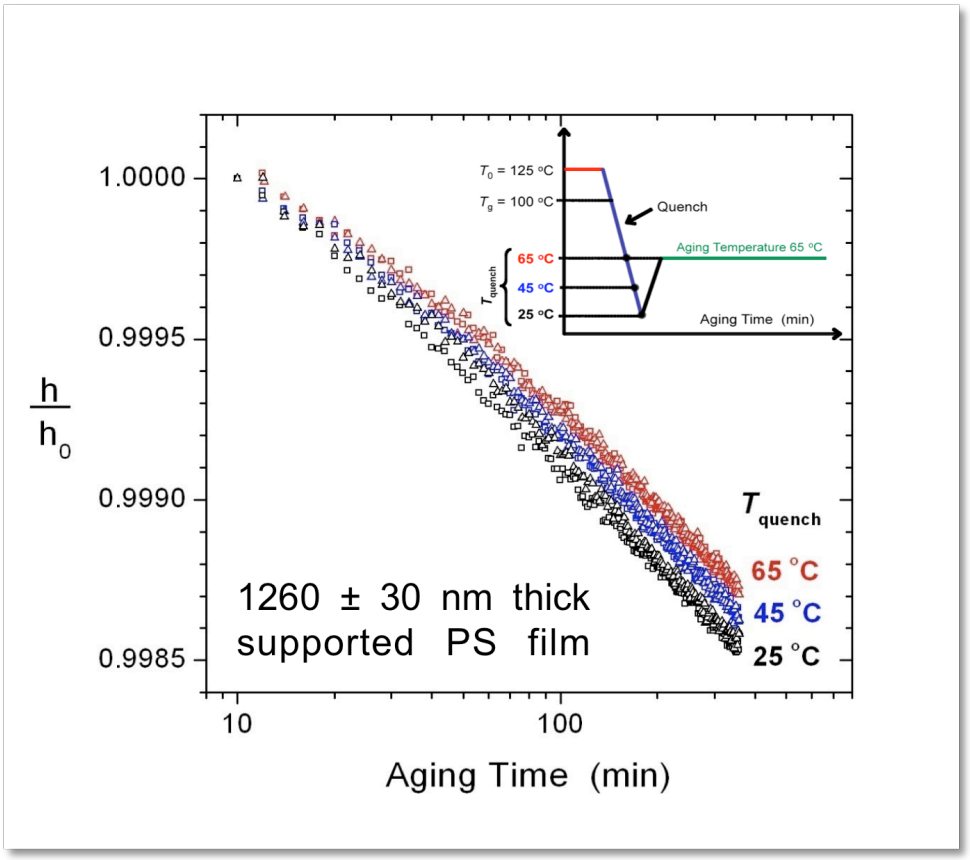

Figure 17. Semilog plot of normalized film thickness h/h_0 as a function of aging time for 1260 ± 30 nm PS films quenched to different temperatures. The films were aged for 6 hours at 65°C. The films exhibit higher aging rates with decreasing quench temperature. Films quenched to 25°C, 45°C, and 65°C exhibited aging rates of $\beta = (9.1 \pm 0.2) \times 10^{-4}$, $(8.6 \pm 0.2) \times 10^{-4}$, and $(7.8 \pm 0.1) \times 10^{-4}$, respectively.

Quench Conditions: Quench Rate

Though the effect of quench temperature on aging is clear, this does not explain why a freestanding quench induces accelerated aging rate with decreasing film thickness, since both supported and freestanding films are normally quenched to the same temperature – room temperature. However, changing T_{quench} does affect another thermal parameter during quenching: the cooling rate of the film through T_g. Cooling rate of a supported film is dependent on the thermal gradient, or in case of one-dimensional heat transfer, simply the difference in temperatures between the sample and the thermal mass at T_{quench}. Since annealing temperature is

kept constant at 120°C, decreasing quench temperature means a greater temperature difference between the film and the thermal mass, and thus a larger cooling rate. Based on this, I hypothesized that the larger cooling rate, rather than the lower quench temperature, causes greater physical aging rate. This could explain why thinner freestanding films age faster: freestanding films experience larger cooling rate with decreasing film thickness, but supported films experience constant cooling rate regardless of the thickness[11].

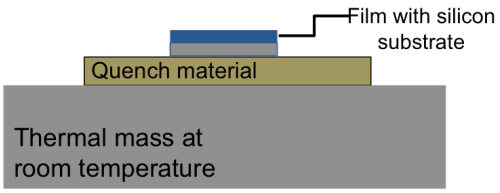

Figure 18. A schematic of the set-up used to cool supported PS films at a different rate. Different quench materials yield different quench rate.

To vary the quench rate without varying the quench temperature, supported PS films were quenched while in full contact with different materials, which I shall refer to as "quench materials": Teflon, stainless steel, and copper, which are themselves in contact with a large thermal mass equilibrated to T_{quench}. Figure 18 shows the schematic of the quench set-up. In this set-up, materials with higher thermal conductivity k more quickly quench the film, but the final quench temperature T_{quench} is kept constant. Figure 19 below is 6-hour aging curves collected by the author using different quench materials. A drastic difference in the aging rates between 980 ± 10nm PS films quenched on Teflon (very low thermal conductivity $k \approx 0.25$ W/m·K, low aging rate) and those quenched on copper (very high thermal conductivity $k \approx 385$ W/m·K, high aging rate) can be observed. However, only a small difference in aging rates is seen between the stainless steel $k \approx 16$~24 W/m·K and the copper, even though the thermal conductivity difference between the two materials is significant.

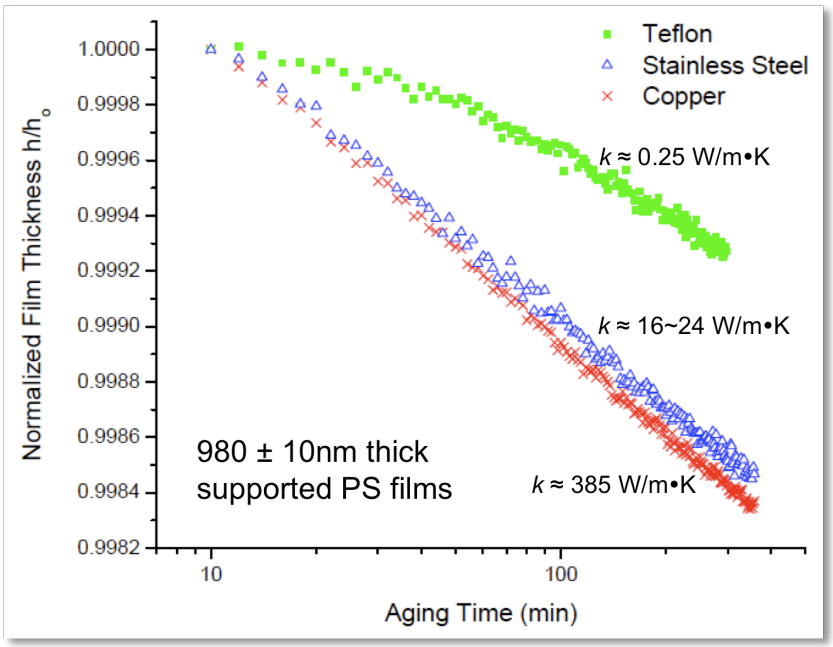

Figure 19. Semilog plot of normalized film thickness h/h_0 as a function of aging time for 980 ± 10 nm thick supported PS films quenched on different materials. The films were aged for 6 hours at 65°C. Three materials, Teflon, stainless steel, and copper with thermal conductivities $k \approx 0.25$, 16-24, and 385 W/m•K were used. Aging rate seems to increase with thermal conductivity of quench materials used to quench the PS film, strongly suggesting that aging increases with quench rate.

These data suggest that physical aging rate increases with increasing quench rate, since thermal conductivity is proportional to the quench rate. Laura Gray in Gray *et al.*[11] tested this more quantitatively by controlling the cooling rate from 1 to 135°C/min using different quench materials or combination of quench materials, with the 6-hour aging results shown in Figure 20. Indeed, as the quench rate is increased, physical aging rate is increased as well. Gray *et al.* also noted that when the quench temperature T_{quench} is changed while the cooling rate is kept constant, no change in physical aging rate occurs. Also note that the cooling rates shown are not the initial cooling rates of the samples, but rather the cooling rate of the samples through T_g.

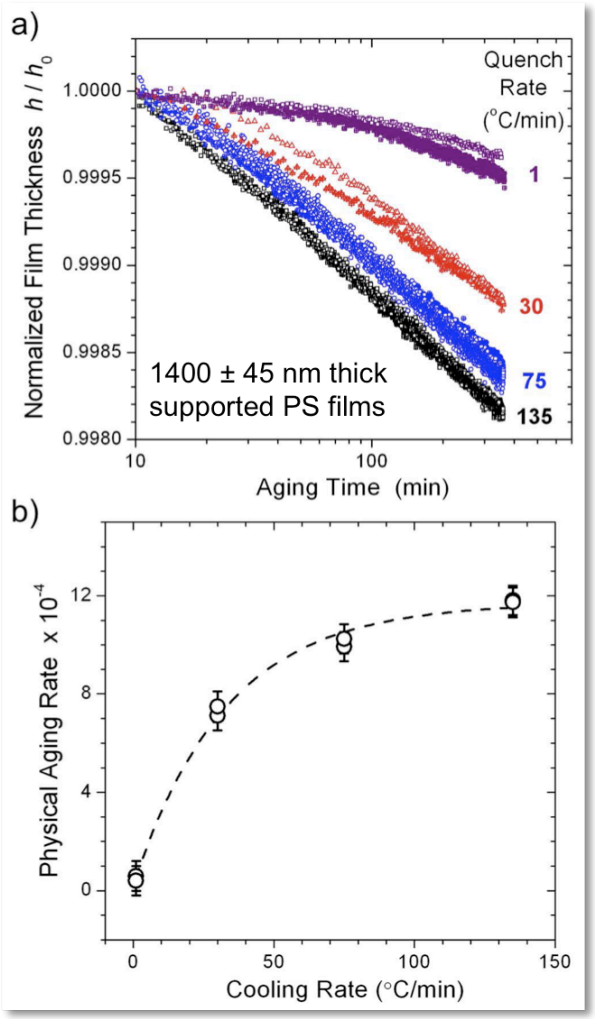

Figure 20. (a) Semilog plot of normalized film thickness h/h_0 as a function of aging time for 1400 ± 45 nm thick PS films supported on silicon demonstrating the effect of cooling rate on the physical aging rate. The films were aged for 6 hours at 65°C. (b) Plot of the measured physical aging rate as a function of cooling rate (reprinted with permission from Laura Gray from ref. 11)

The aging rate, however, does not increase indefinitely. Gray *et al.* notes that the aging rate saturates for quench rates in excess of ~100°C/min, as suggested by Figure 20b. For a typical supported film the quench rate is 50°C/min, while for a typical freestanding film of thickness 400 nm to 1000 nm, the quench rate is ~30000°C/min or greater[11]. Even though the quench rate

increases with decreasing film thickness for freestanding films, since aging rate saturates for quench rates in excess of ~100°C/min at $\beta \approx 12$, all freestanding films should age at a similar rate. However, as we have already noted from Figure 3 in the Introduction section, 600 nm freestanding PS films age faster than 1260 nm freestanding films. In addition, if quench rate is the only cause of observed accelerated aging rate with decreasing thickness behavior, the aging rate of freestanding films quenched at ~30000°C/min should be higher than that of supported films quenched at ~50°C/min. However, β aging rates of 1260 nm and 600 nm thick films quenched supported (9.5×10^{-4} and 9.3×10^{-4}, respectively) are higher than those quenched freestanding (6.0×10^{-4} and 8.1×10^{-4}, as shown in Figure 12), suggesting there might be another quench condition that is affecting the results. Note that when supported films were cooled to various quench temperature with the quench rate kept constant, no change in the aging rate was observed, demonstrating that the quench rate, not the quench temperature, affects the physical aging rate[11].

Free Volume and Potential Energy Landscape Argument

The underlying reason for why cooling (quench) rate strongly affects the aging rate is the relationship between quench rate and thermodynamic stability. When polymer glasses are cooled, molecular motions slow down until vitrification at T_g traps the glasses in an unstable state with excess thermodynamic quantities, such as excess volume. If the cooling is fast enough, the polymer molecules have little time to orient themselves to assume a low volume configuration, "freezing" the glass at a high-volume configuration. Figure 21 demonstrates this behavior. When a glass-forming material is quenched from the liquid equilibrium state more quickly, it begins to deviate from equilibrium at a higher temperature. Thus, a glassy polymer

quenched quickly has more excess volume than that quenched slowly. Since the driving force behind physical aging is the energy difference between the equilibrium state and the glassy state (or the excess thermodynamic quantities)[13], faster cooling rate through T_g leads to faster aging. In addition, excess volume corresponds to a larger free volume available between molecules. The larger free volume implies there are more configurational freedom and mobility for the polymer molecules, which should lead to a larger aging rate.

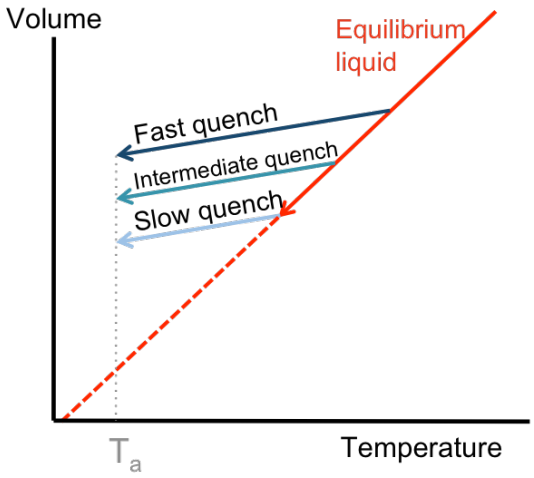

Figure 21. Illustration of excess volume generated with fast quench for a glassy material. Because a fast quench leaves the glass with higher excess thermodynamic quantities, a quickly quenched glass should exhibit a higher aging rate than a slowly quenched glass.

The trapping of glasses in a high-energy state can be qualitatively understood with the concept of a potential energy landscape[14,15]. A potential energy landscape for a glass system can be described as a series of local energy minima and maxima, as Figure 22a demonstrates. Upon cooling from the liquid state, the polymer glass gets trapped in a local potential energy minimum (or energy basin) due to reduced kinetics at lower temperatures, preventing the system from overcoming a local potential energy maximum (transition state) to transition over to a lower energy state. With what thermal energy and mobility is available, the trapped glassy state progresses slowly deeper into the energy minima, which results in physical aging. With the

potential energy landscape picture in mind, we can attempt to qualitatively explain why a faster quench rate yields a higher physical aging rate. Above T_g, most energetic states are accessible to the glass as the molecules have enough kinetic energy to traverse the energy landscape. A slow quench can ease glasses to a lower energy state by providing enough thermal energy for molecules to explore various transition states, but at the same time gradually making the higher energy states inaccessible to the glass as the temperature is decreased. A fast quench traps the glass at a higher energy state, because the drastic decrease in the thermal energy traps the glass at the nearest local energy minimum available. Since higher energy states were available before quenching, a faster quench allows the glass more access to a high-energy state than slower quench does, thus making the glass age faster.

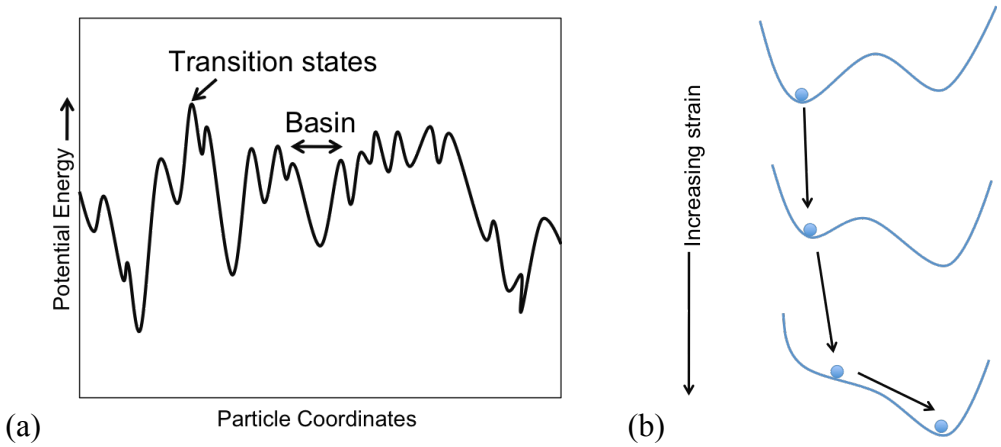

Figure 22. Behavior of polymer films under different thermal and mechanical conditions can be understood with a potential energy landscape picture. (a) Potential energy landscape as described by Stillinger contains basins, or local energy minima, and transition states, or local energy maxima. Glasses can be trapped at one of the local energy minima. Over time, glasses are driven to reach a lower energy, and this drive manifests as physical aging. (b) Lacks and Osborn proposed that the potential energy landscape changes when stress or strain is applied to the glass. This can affect aging behavior by making previously inaccessible energy states now accessible (Figure (a) based on ideas presented in ref. 15 and Figure (b) based on ideas presented in ref. 14).

Quench Conditions: Mechanical Stress During Quenching

It is believed that the potential energy landscape can be altered when an external mechanical stress is applied to the glass. Lacks and Osborn[14] demonstrate with computer molecular simulations how the shear strain (lateral deformation due to applied shear stress) can alter the landscape to create new energy maxima and minima, as Figure 22b illustrates. This means changes in energy landscape due to a mechanical stress may have an effect on the physical aging rates by allowing access to a previously inaccessible energy states. More importantly, the Roth lab hypothesizes that stress applied *during* vitrification may lock the glass in a different energy minimum, causing the glass to behave differently. In my experiments and those in Gray *et al.* (refer back to Figure 12), both supported and freestanding films experience unintended mechanical stresses due to thermal expansion mismatch between the film and the silicon substrate or, in the case of freestanding films used in Gray *et al.*, the steel wire frames. Moreover, stress build-up upon quenching for films quenched supported is independent of thickness while that for films quenched freestanding increases with decreasing thickness, suggesting a possible trend between stress and physical aging[11].

A thermal expansion coefficient is a measure of the amount of the expansion of a material upon heating. When quenching, the silicon substrate and the PS film experience different contraction rates because the PS film has a larger thermal expansion coefficient than the silicon. Since the film is bound to the silicon substrate, quenching will result in biaxial stress and strain along the plane of the film, leading to a stress buildup upon cooling below T_g[16]. The stress that builds up on a supported film upon quenching is calculated as follows[17]:

$$\sigma_{PS} = \frac{E_{PS}}{1 - \nu_{PS}}(\alpha_{PS} - \alpha_{Si})\Delta T$$

where σ_{PS} is mechanical stress on the PS film, α_{PS} and α_{Si} are the thermal expansion coefficients

of PS and silicon substrate, respectively, E_{PS} is the elastic modulus for PS, ν_{PS} is the Poisson's ratio for PS, and ΔT is the temperature change. Note that, since the elastic modulus, the Poisson's ratio, and the thermal expansion coefficient are all temperature dependent, the above equation should be formally regarded as an integral with respect to T. Also note that because α_{PS} is ~2 orders of magnitude greater than α_{Si}, it is common to treat $\alpha_{Si} \approx 0$ to omit the term from the equation.

Normally, ΔT is regarded as the temperature difference between the final temperature and the initial temperature of the cooling process, which in our case would be the annealing temperature (120°C, since we are using PS films) and T_{quench}, respectively. However, Zhao *et al.* has previously demonstrated that no stress builds up above T_g[16], because polymer films above T_g are equilibrium liquids. This is consistent with my observation that varying the annealing temperatures from 110°C to 170°C has no effect on the aging rate of the PS film (refer back to Figure 17). Thus, we should regard ΔT as the temperature difference between T_{quench} and T_g. Based on the stress equation above, we calculate that the tensile stress imparted to a PS film supported on a silicon substrate is ~12 MPa, with no dependence on film thickness[11]. This is in the same order of magnitude with 15 MPa as measured by Chung *et al.*[18] for a PS film cooled while supported on mica.

For the freestanding film preparation, the PS films are draped across a rectangular wire frame made of stainless-spring steel wire, attached to the wire frame on the two sides. Upon quenching, the PS films contract faster than the wire frame, causing stress. Although it is not possible to directly calculate the stress imparted to the film by the wire frame, several observations can help understand qualitatively how much stress is being applied to the film. The steel wire frame flexes slightly as the film becomes taut upon annealing above T_g; thus, the wire

frame effectively acts as a small spring with an effective spring constant *k* that applies some force $F = kx$ corresponding to the amount of the displacement of the wire frame, *x*.[11] The uniaxial tension along the length of the film of thickness *h* imparts a stress corresponding to $\sigma = F / A = F /(hw)$, where *w* is the width of the film. Unfortunately, the amount of displacement of the wire frame was too small to measure directly. Since stress is inversely proportional to the thickness of the film, we can expect the stress on the film to increase as the film thickness *h* decreases.

Studies on the effects of stress during quenching have not been directly done before. However, Shelby and Wilkes[19] have studied uniaxially hot drawn PS and polycarbonate (PC) samples. This was to study the effects of molecular orientation induced by uniaxial stretching on the physical aging rate of polymers. Hot drawn PS is prepared by elongating bulk PS above T_g then cooling them under tension. It was found that a PS film displays around a 50% faster aging rate upon stretching[19].

In order to study the effect of the stress during quenching on the film, a lever system designed to impart stresses on the freestanding PS films was constructed by Laura Gray, as explained in the Experimental Procedures section. The experimental details are listed in the Experimental Procedures section. Stresses applied to the film during quenching are adjusted by varying the weight added to the lever system. Masses used are 0g, 5g, 7g, 10g, 15g, 20g, 30g, 40g, and 50g, corresponding to stresses from 0 MPa to 13.5 MPa on the film (for example: $\sigma = mgd_1 / hwd_2$, so σ=0.050kg*9.81m/s^2*46.37mm/(1660*10^{-9}m*10^{-2}m*101.25mm)=13.5MPa) In Figure 23 below, 3-hour aging curves for 1660 ± 30 nm thick PS films under stress from only the weights 5g, 15g, 20g, and 50g are shown. Other aging curves were not included to reduce confusion. Significant noise can be observed, with little to no observable trend.

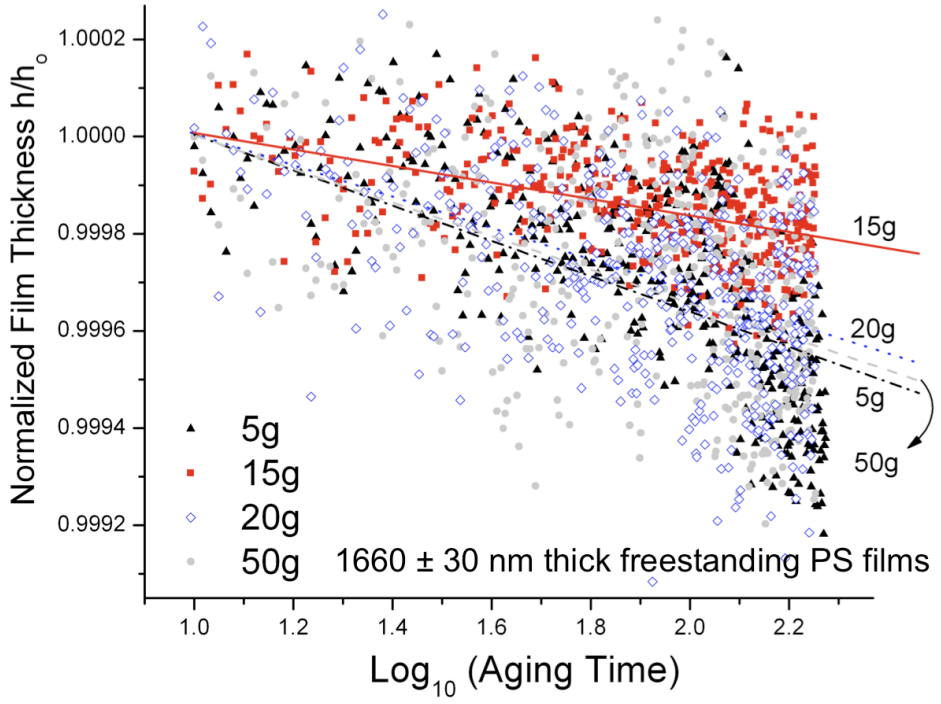

Figure 23. Plot of normalized film thickness h/h_0 with respect to $\log_{10}$ of aging time for 1660 ± 30 nm thick PS films quenched freestanding under various stresses from weights placed onto the lever system. These films were aged for 3 hours at 65°C. Significant noise can be seen.

Given the amount of noise in these data, in order to obtain the aging rates and representative errors from this data, I devised a procedure described in Figure 24. A line was drawn by hand to indicate "lower bound" aging rate and "upper bound" aging rate, so that approximately 2/3 of the points above or below the computer-generated linear fit of the curve lie between the fit and the hand-drawn line. The slope of the upper and lower bound lines were then measured. The standard deviation σ_β of aging rate was taken to be the half the difference between the upper bound and the lower bound aging rates. The linear fit of the data was taken to be the mean aging rate. The error calculated this way should be representative of the real error because, in a Gaussian distribution, one standard deviation from the mean value spans 68% (about 2/3) of a given data set. Note that all these lines were restricted so that they pass through

the coordinate (1,1) because the film thickness is normalized at 10 minutes when $\log_{10}$(Aging Time) = 1 is the x-coordinate. Also note that the x-coordinate was converted to a linear plot with respect to $\log_{10}$(Time) because this allows easier calculation of the slope of the upper and lower bound lines.

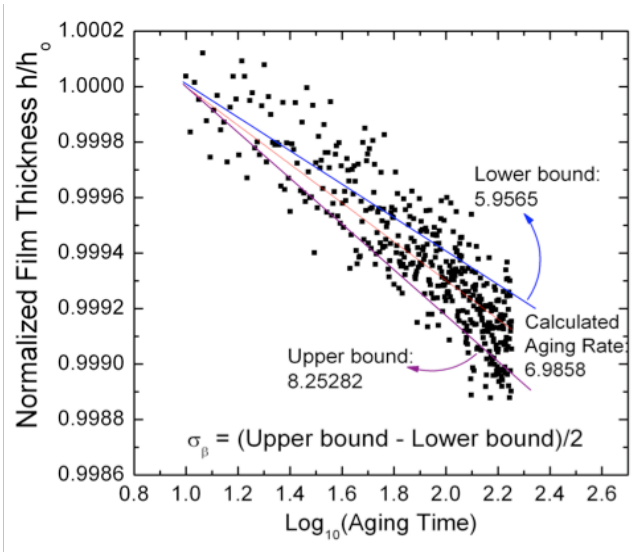

Figure 24. Calculation of error for noisy aging data. Lower bound (blue line) was estimated by drawing the line so that 2/3 of the points above the linear fit of the data (red line) are between the blue and red lines. Upper bound (purple line) was estimated by drawing the line so that 2/3 of the points below the linear fit of the data are between the purple and red lines. The slopes of the lines were then measured. The error σ_β was calculated by taking the difference between the upper and lower bound aging rates then dividing it by 2.

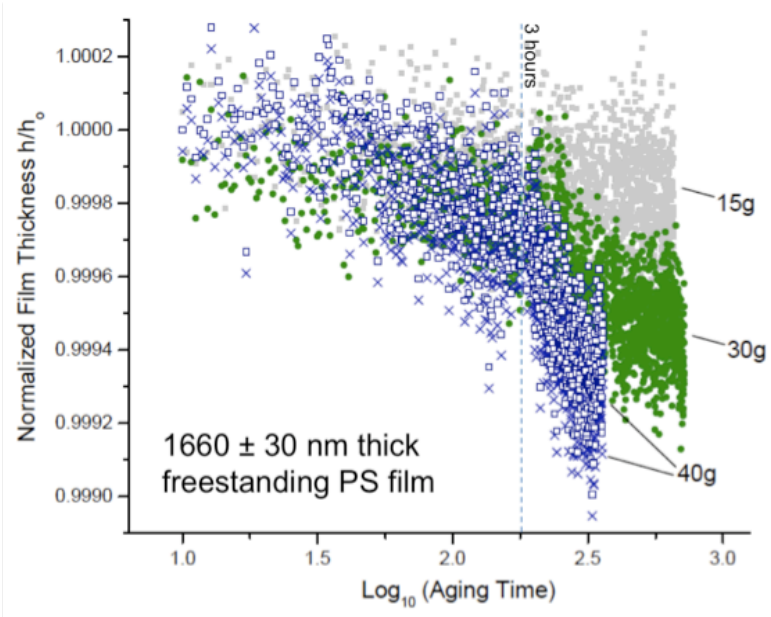

Figure 25. Normalized film thickness h/h_0 versus $\log_{10}$ of aging time for freestanding PS films 1660 ± 30 nm thick illustrating the anomalous aging behavior of the films stressed with a lever system. The films were aged at 65°C for 6 or more hours. The films more or less maintain their thickness until after 3 hours of aging (corresponding to x-coordinate of 2.25), when their thickness abruptly decreases. It appears as though increasing the mass causes a more rapid drop in thickness, suggesting a higher aging rate for higher masses.

A compilation of aging rates (with error bars) as a function of weight used to apply stress to the 1660 ± 30 nm thick PS films during quenching using the lever system is shown in Figure 25. A total of 11 films were tested. Although a trend seems to occur where physical aging rate

increases with increasing weight, the error bars often overlap each other, making it hard to state with confidence that a trend occurs. Moreover, many of the films under higher stresses exhibited a strange but reproducible behavior where they more or less maintained their thickness until after around three hours of aging, after which the aging rate increased rapidly, as if a delayed aging occurred. This behavior made it difficult to fit the aging curve to a line. Figure 25 illustrates this behavior. A small trend can be seen where the drop in thickness is intensified with increasing mass, weakly suggesting that aging increases with stress. Note that two sets of 40g data were used to illustrate the reproducibility of this phenomenon.

The lever system designed to apply different stresses to the freestanding films during the thermal quench had additional difficulties. Occasionally, static friction in sliding portion of the sample holder reduced the amount of tension being applied to the PS film. The friction was sometimes so great that even when a 50g weight was used, the sliding portion of the sample holder did not budge. The stress that would be applied to the PS film by a 50g weight is 13.5 MPa. When a 10g of mass corresponding to 6.54 MPa was directly hung to a film with cross-sectional area 1500 nm × 1.0 cm (the technique of which is described in the following section) during annealing, the film stretched and then broke within a minute; this indicates that some amount of static friction is preventing the intended stress to be fully applied to the film. Thus, the data in Figure 26 should thus be scrutinized with care, but not all of the data here should be completely disregarded; even though the exact amount of stress cannot be quantified, higher weight still implies a relatively larger stress on the film.

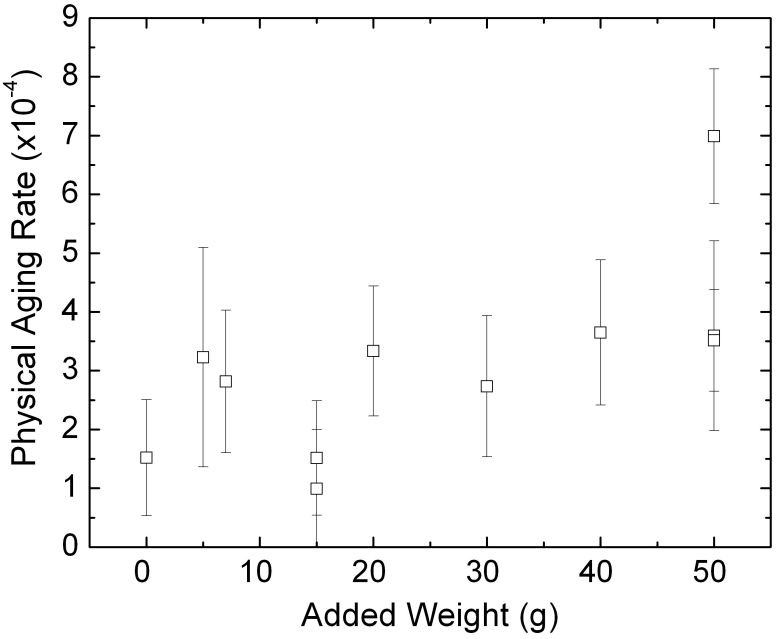

Figure 26. Physical aging rate with respect to added weight for 1660 ± 30 nm freestanding PS films. A weak positive correlation between the added weight and the aging rate can be seen. These results should not be taken at face value because of the high static friction in the instruments preventing the full tension to be applied to the PS film.

Directly Hanging Mass to PS Film

In order to make sure all the stress is being applied to the film, I developed a technique in which a mass is directly hung on one end of a polystyrene film. This would eliminate all concerns about the static friction in the lever system. These films are prepared in the same way that the freestanding films are prepared, except with one extra step of taking the film out of the water onto a flat surface (stainless steel plate) in order to attach a mass. The film is then floated back onto water before it is picked up again with the sample holder used in the lever system so that the side of the film with no mass attached is in contact with the sample holder. Figure 27 is a picture of the sample. The masses hung on the film are square pieces of Teflon of mass 0.0326g, 0.0779g, and 0.251g, which correspond to stresses σ (calculated by dividing the weight, *mg*, of

the masses by the *cross-sectional* area of the film, $A=hw$; so $\sigma=mg/hw$, where h is thickness of the film and w is width of the film) of 0.0320 MPa, 0.0764 MPa, and 0.2458 MPa for 1000 ± 10 nm thick PS films (with width w = 1.0 cm) used in my experiments. Just as with the lever system experiments, the floated film is then put in the heating chamber for annealing. During annealing above T_g, the mass on the end of the PS film is supported so that no stress is applied to the film. A minute before quenching, the sample holder is adjusted such that the mass hangs freely from the end of the film. This ensures that the stress is applied only during the thermal quench. The film is then quenched by opening the heating chamber and allowing room temperature air to flood the chamber by leaving it open for 1 minute. The results of these experiments are shown in Figure 28. It is noteworthy that these films, unlike other freestanding films, did not thicken because no stress was being applied to the films during the majority of the time in which films were annealed above T_g.

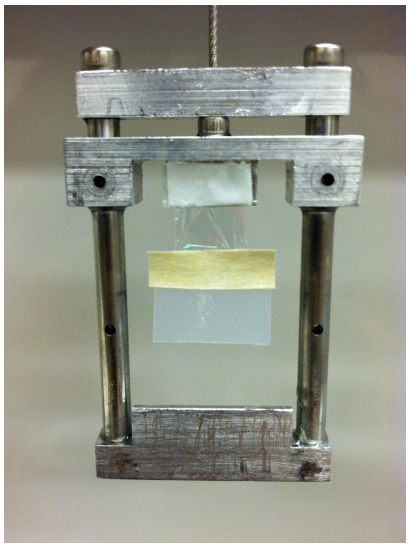

Figure 27. Picture of Teflon mass (0.0326g) hanging on a 1000 nm PS film. The mass is attached to one side of the film with an adhesive, and the other side is hung on the sample holder as shown.

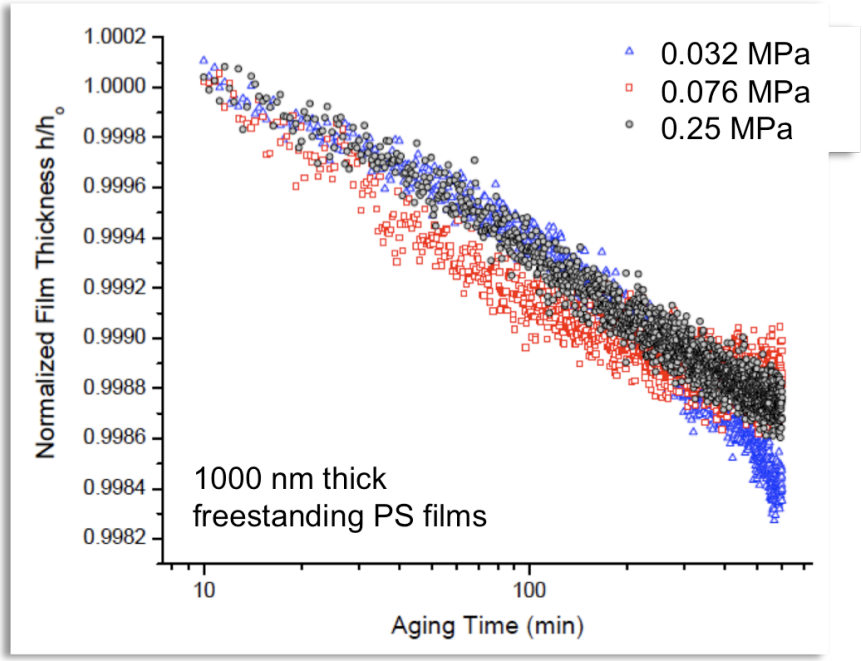

Figure 28. Semilog plot of normalized film thickness h/h_0 as a function of aging time for 1000 ± 50 nm thick PS films quenched freestanding with a mass hung on the end. The films were aged for 12 hours at 65°C. The aging rates for films under 0.0320, 0.0764, and 0.2458 MPa of stress were $\beta = 7.87 \times 10^{-4}$, 7.21×10^{-4}, and 7.08×10^{-4}, respectively. These aging rates are not significantly different from each other, and the curves collapse onto one graph. The applied stress is very small, so no definite relationship between stress and aging can be implied here.

The aging rates for films hung with 0.0326g, 0.0779g, and 0.251g of mass were $\beta = 7.87 \times 10^{-4}$, 7.21×10^{-4}, and 7.08×10^{-4}, respectively. These aging rates are not significantly different from each other, and the aging curves are essentially on top of each other. This graph may lead the reader to conclude that stress has no effect on the aging rate; however, it is important to keep in mind that the stresses applied to the films here (0.0320 - 0.2458 MPa) are miniscule compared to the stress experienced by supported PS films, which is on the order of ~12 MPa.[11] This means that the variation in the amount of stress in these experiments may be too small to observe any trend in the aging rate. I have attempted to increase the stress by using heavier masses, but this required the use of adhesives to keep the masses from falling off the film and to keep the films from falling off the sample holder. The high temperature conditions of annealing frequently

made the adhesives fall off, making it difficult to apply higher stresses to the film. Though higher stresses could not be applied, this graph is significant because of the reproducibility of the aging rates and how well the data agree with each other.

In light of the fact that the freestanding films used in our experiments undergo an extremely fast quench, a prediction could be made about how the aging rate should behave with increasing stress, if stress indeed is the cause of the accelerated aging behavior. According to Gray *et al.* [12], the aging rates for *supported* PS films quenched at 100°C/min or higher saturates at around $\beta \approx 12 \times 10^{-4}$. The freestanding PS film cools beyond this saturation rate, at around ~30000°C/min. Since about ~12 MPa of stress builds up in a supported film during quenching, if the stress due to a hanging weight could be increased to the order of ~10 MPa, we should observe aging rates of around $\beta \approx 12 \times 10^{-4}$.

Directly Hanging Mass to PS Film During Annealing: Preliminary Results

Ordinarily, when a freestanding film is prepared its thickness increases during annealing[11,6]. In this thesis we see when a film is prepared so that no force is directly applied to the film during the annealing process, as with freestanding films used in the Directly Hanging Mass to PS Film subsection, films do not thicken. The three films used in the subsection above were prepared to be 1000 nm thick before annealing (solution: 9% PS by weight in toluene spun at 3000 rpm), and these films yielded post-annealing thicknesses of 971, 1034, and 977 nm. Thus it can be assumed that the freestanding PS films used in Gray *et al.*[11] and Huang and Paul[6] were stretched during annealing. In order to quantify the effect of hanging weight during annealing on film thickening, three freestanding PS films spun to be 1000 nm and two films spun to be 1500

nm thick (before annealing) were prepared in the same manner as the films in the previous subsection by hanging Teflon masses on the films. The difference was that the masses were hung on the film during the entire annealing and quenching process, not only 1 minute during annealing and quenching. It was found that the three films targeted to be 1000 nm thickened to 1240, 1263, and 1243 nm when 0.0595, 0.0856, and 0.0853 g of Teflon, respectively, were hung. These correspond to 24-26% increase in film thickness. The two films targeted to be 1500 nm thickened to 2910 and 1847 nm when 0.0304 and 0.0984 g of mass, respectively, were hung. These correspond to 96% and 23% increase in film thickness.

One of the difficulties with freestanding films draped across a thin wire frame as used by Gray *et al.* is that the actual stress applied to the freestanding film is not directly measurable. I suggest that one could quantify such stress by searching for a hanging mass that would thicken the films the same amount as annealing the films on a thin wire frame. In Gray *et al.* the films thickened from 730 ± 40 nm to 1200 ± 100 nm, corresponding to a 64% increase in film thickness. A mass that would thicken a 730 nm film to 1200 nm, if found, would be useful in calculating the actual stress applied to the freestanding films during annealing and quenching.

CONCLUSIONS

Thin freestanding polysulfone (PSF) films 400 nm to 4000 nm thick have previously exhibited an increased aging with decreasing film thickness behavior according to gas permeation studies, but thin supported polystyrene (PS) films 100 nm to 2500 nm thick have

previously exhibited no change in aging rate with decreasing film thickness. In this thesis we resolve this contradiction by showing that if PSF films are prepared supported, not freestanding, no change in aging rate occurs with decreasing film thickness. Various quench conditions that affect the aging rate of thin polymer films are then examined. In particular, effects of mechanical stress during quenching and thermal conditions, such as annealing temperature, quench temperature, and quench rate through T_g were examined. It was shown that the aging rate of supported thin film PS increases with increasing cooling rate of the supported PS film, and that the quench temperature T_{quench} – unless the temperature increases the cooling rate – and annealing temperature do not affect the physical aging rate. The increased aging rate behavior of the film with increasing cooling rate was justified with a free volume and a potential energy landscape argument. Specifically, it was noted that a fast quench could trap glasses at a higher volume and energy state than a slow quench. Based on the suggestion that the potential energy landscape can be altered with stress and strain, we propose a possibility that stress during the thermal quenching process may trap glasses in a different energetic state, inducing a different aging behavior than would be expected of quenched films without stress. We hypothesize that, since thinner freestanding films – which undergo faster aging – experience a larger stress than thicker freestanding films, aging rate i5ncreases may correlate with applied stress. Initial data indicate that this may be true; however, more data at higher stresses must be collected before any conclusive relationship can be drawn between stress and physical aging rate.

REFERENCES

1. Larson, R., *The Structure and Rheology of Complex Fluids (Topics in Chemical Engineering)*. Oxford University Press, USA: 1998.
2. Struik, L. C. E., *Physical aging in amorphous polymers and other materials*. Elsevier Scientific Pub. Co.: 1978.
3. Priestley, R. D. *Soft Matter* **2009**, *5*, 919-926. *Physical aging of confined glasses*.
4. Huang, Y.; Paul, D. R. *Polymer* **2004**, *45*, 8377-8393. *Physical aging of thin glassy polymer films monitored by gas permeability*.
5. Koros, W. J.; Fleming, G. K. *Journal of Membrane Science* **1993**, *83*, 1-80. *Membrane-based gas separation*.
6. Huang, Y.; Paul, D. R. *Macromolecules* **2006**, *39*, 1554-1559. *Physical Aging of Thin Glassy Polymer Films Monitored by Optical Properties*.
7. Tompkins, H.; Haber, E., *Handbook of Ellipsometry (Materials Science and Process Technology)*. William Andrew: 2006.
8. Hecht, E., *Optics (4th Edition)*. Addison Wesley: 2001.
9. Baker, E. A.; Rittigstein, P.; Torkelson, J. M.; Roth, C. B. *Journal of Polymer Science Part B: Polymer Physics* **2009**, *47*, 2509-2519. *Streamlined ellipsometry procedure for characterizing physical aging rates of thin polymer films*.
10. Pye, J. E.; Rohald, K. A.; Baker, E. A.; Roth, C. B. *Macromolecules* **2010**, *43*, 8296-8303. *Physical Aging in Ultrathin Polystyrene Films: Evidence of a Gradient in Dynamics at the Free Surface and Its Connection to the Glass Transition Temperature Reductions*.

11. Gray, L. A. G.; Yoon, S. W.; Pahner, W. A.; Davidheiser, J. E.; Roth, C. B. *Macromolecules* **2012**, *45*, 1701-1709. *Importance of Quench Conditions on the Subsequent Physical Aging Rate of Glassy Polymer Films*.

12. Hall, D. B.; Underhill, P.; Torkelson, J. M. *Polymer Engineering & Science* **1998**, *38*, 2039-2045. *Spin coating of thin and ultrathin polymer films*.

13. Hutchinson, J. M. *Progress in Polymer Science* **1995**, *20*, 703-760. *Physical Aging of Polymers*.

14. Lacks, D. J.; Osborne, M. J. *Physical Review Letters* **2004**, *93*, 255501. *Energy Landscape Picture of Overaging and Rejuvenation in a Sheared Glass*.

15. Stillinger, F. H. *Science* **1995**, *267*, 1935-1939. *A Topographic View of Supercooled Liquids and Glass Formation*.

16. Zhao, J.-H.; Kiene, M.; Hu, C.; Ho, P. S. *Applied Physics Letters* **2000**, *77*, 2843-2845. *Thermal stress and glass transition of ultrathin polystyrene films*.

17. Benham, P. P.; Crawford, R. J.; Armstrong, C. G., *Mechanics of Engineering Materials, 2nd ed.* Addison Wesley Longman: London, 1996.

18. Chung, J. Y.; Chastek, T. Q.; Fasolka, M. J.; Ro, H. W.; Stafford, C. M. *ACS Nano* **2009**, *3*, 844-852. *Quantifying Residual Stress in Nanoscale Thin Polymer Films via Surface Wrinkling*.

19. Shelby, M. D.; Hill, A. J.; Burgar, M. I.; Wilkes, G. L. *Journal of Polymer Science Part B: Polymer Physics* **2001**, *39*, 32-46. *The effects of molecular orientation on the physical aging and mobility of polycarbonate—solid state NMR and dynamic mechanical analysis*.